processes

MDPI

Article

Equation of State Associated with Activity Coefficient Model Based on Elements and Chemical Bonds

Xinyu Li [1], Baowei Niu [1], Wenjiao Ma [2], Wenying Zhao [3], Xiaoyan Sun [1], Li Xia [1,*] and Shuguang Xiang [1]

[1] Institute of Process System Engineering, College of Chemical Engineering, Qingdao University of Science and Technology, Qingdao 266042, China; 2020010021@mails.qust.edu.cn (X.L.); 02796@qust.edu.cn (B.N.); sun_xyan@163.com (X.S.); xsg@qust.edu.cn (S.X.)
[2] College of Chemistry and Chemical Engineering, Ningxia Normal University, Guyuan 756000, China; 82012016@nxnu.edu.cn
[3] Chemistry and Chemistry Engineering Faculty, Qilu Normal University, Jinan 250200, China; qdzhaowenying@163.com
* Correspondence: xiali@qust.edu.cn

Abstract: A new element- and chemical bond-dependent G^E-EoS model(SRK-UNICAC) is proposed to consider the deviation of the vapor and liquid phases from the ideal state. The SRK-UNICAC model combines the UNICAC model and the SRK cubic equation of state. It uses the original interaction parameters of the UNICAC model and uses this model to calculate the G^E. The SRK-UNICAC model predicted vapor-liquid equilibria for 87 binary systems under low- and medium-pressure conditions, 12 binary systems under high-pressure conditions, and 14 ternary systems; a comparison of the predictions with five other activity coefficient models were also made. The new model predicted the vapor-phase fraction and bubble-point pressure, and temperature for the binary system at high pressure, with a mean relative error of 3.75% and 6.58%, respectively. The mean relative errors of vapor-phase fraction and bubble-point temperature or bubble-point pressure for ternary vapor–liquid phase equilibrium were 6.50%, 4.76%, and 2.25%. The SRK-UNICAC model is more accurate in predicting the vapor–liquid phase equilibrium of high-pressure, non-polar, and polar mixtures and has a simpler and wider range of prediction processes. It can therefore be applied to the prediction of vapor–liquid equilibrium.

Keywords: elements; chemical bonds; G^E-EoS; vapor-liquid equilibrium; SRK-UNICAC

Citation: Li, X.; Niu, B.; Ma, W.; Zhao, W.; Sun, X.; Xia, L.; Xiang, S. Equation of State Associated with Activity Coefficient Model Based on Elements and Chemical Bonds. *Processes* **2023**, *11*, 1499. https://doi.org/10.3390/pr11051499

Academic Editor: Andrew S. Paluch

Received: 7 April 2023
Revised: 29 April 2023
Accepted: 9 May 2023
Published: 15 May 2023

1. Introduction

One of the important components of chemical data is vapor-liquid phase equilibrium(VLE) data. VLE data are required for most unit operations, chemical designs, separation studies, process optimization, etc. VLE is of great value for both theoretical chemical research and practical applications. In today's increasingly complex and large-scale production processes, it is impossible to obtain all the required data experimentally due to the high workload and cost of experimental determination of VLE data; therefore, obtaining VLE by thermodynamic model estimation is becoming increasingly more significant.

The equation of state(EoS), the activity coefficient model, and the excess Gibbs free energy-equation of state model(G^E-EoS model) are three commonly used methods to calculate the VLE. EoS expresses the relationship between temperature, pressure, and molar volume of a substance [1], and has an important position in the calculation of VLE and gas-liquid phase equilibrium(GLE), especially in the calculation of phase equilibrium at medium and high pressures. The activity coefficient model has wide applications in low-pressure VLE, liquid-liquid phase equilibrium(LLE), and vapor–liquid–liquid phase equilibrium(VLLE). However, the activity coefficient model requires different parameters at different temperatures when calculating strongly non-ideal systems and can only be used for the liquid phase. Due to the lack of interaction parameters at high pressure, the

activity coefficient model is only applicable to low-pressure conditions. The cubic equation of state is usually chosen to predict the VLE of the system at high pressure. Although EoS can be used for calculations in a larger temperature and pressure range, the accuracy of calculations for strong non-ideal systems and the critical region and above the critical region is sometimes still insufficient. The newly developed G^E mixing rule in recent years introduces the activity coefficient model for the liquid phase into the expression of EoS, combining EoS and the activity coefficient model in a new way. The G^E-EoS model can be used for phase equilibrium calculations over a larger temperature and pressure range, for more systems, and with better computational accuracy.

Huron and Vidal [2] (1979) first used the excess Gibbs function in combination with EoS to obtain a new type of mixing rule, the Huron-Vidal(HV) mixing rule, which gives significantly better results than the van de Waals single-fluid mixing rule when polar mixtures are calculated using this mixing rule. In 1992, the Wong-Sandler mixing rule(WS) using infinite pressure as the reference state was proposed [3]. In contrast to the HV mixing rule, the WS mixing rule uses A^E instead of G^E and introduces a second virial coefficient in b. This allows both the direct use of the existing parameter list of the activity coefficient model and compliance with the boundary conditions of the second virial coefficient. Feroiu and Geana [4] (1996) proposed the Huron-Vidal infinite dilution(HVID) model by a combination of the HV mixing rule with the Soave–Redlich–Kwong(SRK) equation. Favorable results were obtained by predicting the phase equilibrium behavior of six groups of binary systems, such as isopropanol–water, over a wide temperature range and pressure range. Iwai [5,6] (2018, 2019) proposed a new activity coefficient model combining the HV mixing rule and the Peng-Robinson(PR) equation of state. It was also demonstrated that the model came to have improved accuracy in predicting the VLE of hydrocarbon–alcohol systems. Yang et al. [7] (2019) predicted the phase equilibrium of the CO_2-H_2O system by WS mixing rules and PR EoS with non-random two-liquid(NRTL) parameters to obtain predictions in high agreement with experimental data.

It is impossible to obtain the critical properties and eccentricity factors of all mixtures experimentally due to the small amount of experimental data on eccentricity factors and critical properties of mixtures. Most of the mixtures involved in industrial production are multi-component mixtures. Therefore, EoS is limited in its application to the calculation of the VLE of mixtures. The mixing rule is a relational equation between the properties of the pure components and the properties of the mixture. The application of EoS in the industry is extended by predicting the properties of mixtures from the properties of pure substances. The HV mixing rule and WS mixing rule are both G^E mixing rules with infinite pressure as the reference state. Lermite and Vidal [8] (1988) combined the HV mixing rule with EoS SRK/PR, respectively, to predict bubble-point pressure and vapor phase composition for hundreds of binary systems containing hydrocarbons and aromatic hydrocarbons, with relative errors within 5% for the vast majority of systems. Haghtala and Espanani [9] (2004) applied the PRSV equation of state in combination with the WS mixing rule to the prediction of VLE for polymer solutions of different molecular weights and obtained results that were consistent with experimental data. Michelsen et al. [10,11] (1990) improved the initial G^E mixing rule with zero pressure as the reference state. They improved the function on α by approximating it as a first-order function and a second-order function and proposed the Huron-Vidal of order 1(MHV1) and Huron-Vidal of order 2(MHV2) mixing rules.

The G^E-EoS model with zero pressure as the reference state only began to be widely used in the calculation of phase equilibria. Holderbaum and Gmehling [12] (1991) proposed the predictive Soave–Redlich–Kwong(PSRK) model using the SRK equation combined with the universal quasi-chemical functional group activity coefficient(UNIFAC) model and the MHV1 mixing rule.

In addition to infinite pressure and zero pressure, there are a number of G^E mixing rules with no defined pressure reference state. Boukouvalas et al. [13] (1994) proposed a linear combination of G^E mixing rules for infinite and zero pressure, known as the linear combination of Vidal and Michelsen(LCVM) mixing rules.

The required parameters for the existing Wilson, NRTL, UNIQUAC, and other activity coefficient models have to be obtained based on binary VLE data. Notably, these data are not readily available. The determination of VLE data requires a lot of human and material resources, and it is impossible to measure every pair of binary VLE data. However, activity coefficient models based on group contributions, such as the UNIFAC model, can possess the ability to predict the VLE without collecting complete binary GLE data, using only the chemical structure of the components in the solution. The activity coefficient model based on group contributions requires only a limited number of group parameters to predict the VLE for a large number of unknown systems. The ASOG model, UNIFAC, and their modified models are unable to obtain some VLE data required by the industry due to the lack of necessary groups required for splitting compounds and the lack of group-interaction parameters, which limits their applications. Therefore, improving the prediction progress of the G^E-EoS model by improving the activity coefficient model is a reliable method. Xia et al. (2022) [14] established a new activity coefficient model named the 'Universal Quasi-Chemical elements and chemical bonds Activity Coefficient'(UNICAC) by regression to obtain the interaction-energy parameters of 10 elements and 33 chemical bonds. The model is based on the UNIQUAC model and uses elements such as C, H, O, N, S, Si, F, and Cl and chemical bonds such as C-C bonds and C-O bonds as the basic contributing units, with simple group splitting.

A new G^E-EoS model(SRK-UNICAC) was developed by combining the UNICAC activity coefficient prediction model and the SRK cubic equation of state. The prediction range of the G^E-EoS model was extended from non-polar and polar mixtures at low to medium-pressure conditions to high-pressure conditions. The new model can predict the VLE of non-polar, polar, and high-pressure mixtures, simply by knowing the chemical structure of the components in the system. It makes the prediction process simpler, broader in scope, and more accurate.

2. SRK-UNICAC Model

2.1. Basic Rationale

2.1.1. Group Splitting

Molecular theory shows that a molecule is the smallest unit of a substance that can exist relatively stably and independently and maintain its physicochemical properties. Molecules are formed by combining elements with interacting forces in a certain order and arrangement. Thus, the properties of a substance depend on the nature and number of elements that make up the substance and on the interactions between the elements (i.e., chemical bonds). Similarly, the behavior of a mixture depends on the nature of the molecules and the forces between them.

In 1927, modern chemical bond theories were proposed by Hettler and London. In 1939, Pauling's publication "The Nature of the Chemical Bond" showed that a chemical bond is the mutual combination of atoms in a molecule or a group of atoms due to the electron coordination relationship. The existence of chemical bonds was first confirmed by Hou and Zhu et al. [15] (2001), whose work "Topology of two-dimensional C60 domains" was published in *Nature*. Dimas et al. [16] (2013) published photographs of individual atoms and bonds using non-contact atomic force microscopy. The scientific research above provides a solid theoretical foundation for the establishment of the SRK-UNICAC model.

2.1.2. G^E-EoS Model

The portion of the thermodynamic properties of a solution that exceeds those of an ideal solution under the same composition, T, and P conditions is called the excess function. The thermodynamic concept of such deviations is characterized in chemical thermodynamics by G^E.

G^E can correct the deviation from the ideal system due to the difference in molecular shapes, sizes, and interactions of the components in the liquid mixture. However, the non-ideal nature of the vapor phase under high-pressure conditions is becoming increasingly

evident. The G^E-EoS model is obtained by introducing the excess Gibbs function into the mixing rule corresponding to EoS. The non-idealities of the vapor and liquid phases can be corrected at the same time, and the accuracy of predicting the VLE of nonpolar, polar, and high-pressure mixtures is improved.

Assuming that the pressure tends to infinity or tends to zero, the G^E calculated by the fluid activity coefficient model is the same as the G^E calculated by the cubic equation of state. This is the main principle of the G^E-EoS model.

$$\left(\frac{G^E}{RT}\right)_P^{EoS} = \left(\frac{G^E}{RT}\right)_P^{M} \quad (1)$$

When deriving the G^E-EoS model, it is usually necessary to use several assumptions, such as which reference state pressure to choose. There are currently several types of reference state pressures for G^E-EoS models: infinite pressure as the reference state, zero pressure as the reference state, and no definite pressure reference state, respectively.

The G^E-EoS model still uses the EoS method to predict the VLE of the mixture but uses the G^E mixing rule instead of the vdW single-fluid mixing rule.

2.2. Model Development

Figure 1 depicts the development path of the SRK-UNICAC model in detail.

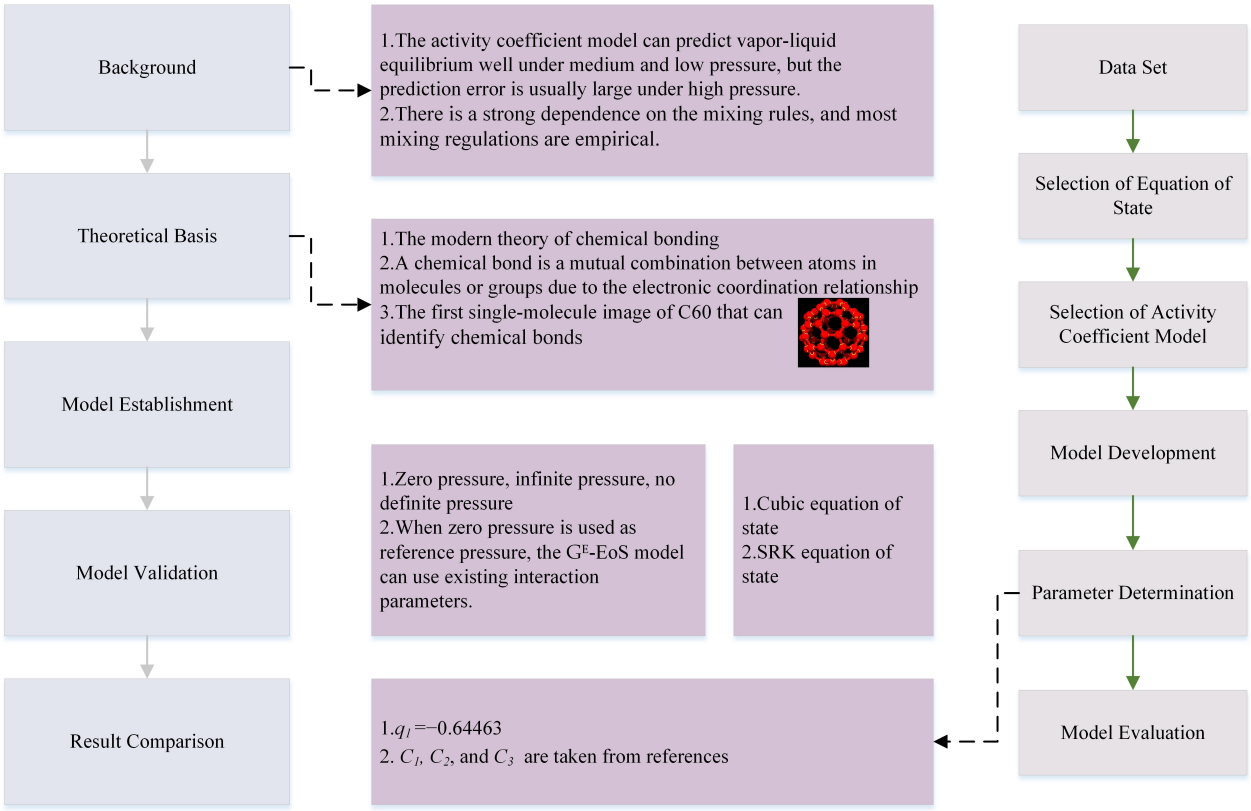

Figure 1. Model construction block diagram.

2.2.1. Reference Pressure Determination

The G^E-EoS model has been developed rapidly since the first G^E mixing rule–HV mixing rule was proposed. There are already some G^E-EoS models applied to the calculation of VLE in industry that have become an important part of chemical process simulation software. In deriving the mixing rule, most assume that the pressure is infinite or zero to simplify the equation. The main mixing rules commonly used include HV, WS, MHV1,

MHV2, PHV, LCVM, HVID, etc. By further examining the derivation process of these hybrid rules, the following results can be obtained:

(1) The G^E mixing rules with infinite pressure as the reference state include the HV, WS mixing rule, etc. Among them, the HV mixing rule can neither meet the boundary conditions of the second virial coefficient nor use the existing parameter table of the activity coefficient model directly. The WS mixing rule has complex cross-interaction parameters k_{ij} and generates a large computational effort when used.

(2) The MHV1, MHV2 mixing rules and PSRK models with zero pressure as the reference state are easy to calculate. Not only can existing interaction parameters be used straight away, but VLE of polar compounds can also be predicted with higher accuracy in a wide range of P, T. Alternatively, the chosen activity coefficient model has a large impact on its prediction accuracy.

It Is clear from the analysis that the G^E-EoS model with zero pressure as the reference state allows the direct application of the parameters of existing activity coefficient models. It also has not only a wide range of P, T applicability but also allows better prediction of phase equilibria of mixtures containing polar compounds. Therefore, the SRK-UNICAC model chooses zero pressure as the reference state. Of course, the prediction results are also closely related to the chosen activity coefficient model. The specific details can be seen in Figure 1.

2.2.2. EoS Determination

EoS is a functional equation describing the P-V-T relationship of a fluid, and it is known from the phase rate that after determining any two of the P, V, and T properties of a pure fluid, the state of the system is also determined. EoS can be used to perform calculations of phase equilibria, e.g., calculating saturated vapor pressure, VLE and LLE of mixtures, etc. EoS is easier and more accurate in the study of phase equilibria of fluids and fluid mixtures, especially in the calculation of VLE under high-pressure conditions.

The SRK equation can be applied to calculate the VLE, which has the advantages of fewer parameters, greater flexibility, and higher accuracy [17]. Most of the G^E-EoS models currently use the SRK equation. Similarly, the SRK-UNICAC model also incorporates it, and the equation of the model with the Mathias–Copeman-modified SRK, as given in Equation (2),

$$P = \frac{RT}{v-b} - \frac{a(T)}{v(v+b)} \tag{2}$$

In the pure component:

$$a(T) = 0.42748 \times \alpha_i(T) \frac{R^2 T_{c,i}^2}{P_{c,i}} \tag{3}$$

$$b = 0.08664 \frac{RT_{c,i}}{P_{c,i}} \tag{4}$$

$$\alpha_i(T) = \left[1 + c_{1,i}(1 - \sqrt{T_{r,i}}) + c_{2,i}(1 - \sqrt{T_{r,i}})^2 + c_{3,i}(1 - \sqrt{T_{r,i}})^3\right]^2 \tag{5}$$

2.2.3. Activity Coefficient Model Determination

Use of 43 elements and chemical bonds as the basic contribution units to the UNICAC model. Since the number of groups is small, it also greatly reduces the possibility of loss of parameters of inter-group interactions.

When using this model to calculate the VLE of a mixture, the prediction range becomes much wider, and the calculation process is much more straightforward. The activity factor is divided into two components, $In\gamma_i^C$ reflects the contribution of the molecular form and size of the pure component i, which is only related to the structure and properties of the pure component and not to the presence of other molecules; $In\gamma_i^R$ reflects the contribution

of intermolecular interactions. The UNICAC model used to calculate the activity coefficient can be seen in Equation (6):

$$In\gamma_i = In\gamma_i^R + In\gamma_i^R \tag{6}$$

The combinatorial term Equation (7) of the UNIQUAC model is used to replace the combinatorial term in Equation (6).

$$In\gamma_i^C = l_i + In\frac{\Phi_i}{x_i} + \frac{zq_i}{2}In\frac{\theta_i}{\Phi_i} - \frac{\Phi_i}{x_i}\sum_{j=1}^{k} x_j l_j \tag{7}$$

The calculation of some parameters in Equation (7) can be expressed as Equations (8)–(10):

$$\theta_i = \frac{q_i x_i}{\sum\limits_j q_j x_j} \tag{8}$$

$$\Phi_i = \frac{r_i x_i}{\sum\limits_j r_j x_j} \tag{9}$$

$$l_i = 5(r_i - q_i) - (r_i - 1) \tag{10}$$

According to the principle of the group contribution method, the parameters r_i and q_i can be obtained from calculating the total sum of the group area contribution and the sum of the group volume contribution.

$$r_i = \sum_i v_k^{(i)} R_k \tag{11}$$

$$q_i = \sum_k v_k^{(i)} Q_k \tag{12}$$

$$R_k = \frac{V_k}{15.17} \tag{13}$$

$$Q_k = \frac{A_k}{2.5 \times 10^9} \tag{14}$$

The residual term is expressed using the residual term of the ASOG model. Molecular interactions are obtained from the summing of the contribution values for each group in the solution:

$$In\gamma_i^R = \sum_k v_k^{(i)} \left[In\Gamma_k - In\Gamma_k^{(i)} \right] \tag{15}$$

The expressions for the activity coefficients Γ_k of the groups k use the equations of the Wilson model:

$$In\Gamma_k = 1 - \sum_l \frac{X_l a_{kl}}{\sum\limits_m X_m a_{lm}} - In\sum_l X_l a_{lk} \tag{16}$$

$$X_i = \frac{\sum\limits_i x_i v_l^i}{\sum\limits_i x_i \sum v_k^i} \tag{17}$$

2.2.4. The SRK-UNICAC Model Derivation

The expression for calculating G^E using the SRK equation is given in Equation (18).

$$\begin{gathered} G^E = RT\left[In(\varphi) - \sum_i x_i In\varphi_i \right] \\ = \frac{1}{RT}\left[(\sum_i x_i \frac{a_i}{b_i} In\frac{V_i + b_i}{V_i}) - (\frac{a}{b} In\frac{V+b}{V}) \right] + \frac{P}{RT}(V - \sum_i x_i V_i) + \sum_i x_i In\frac{V_i - b_i}{V - b} \end{gathered} \tag{18}$$

The fugacity f of the mixture can be calculated from Equation (19):

$$In\frac{f}{P} = z + \frac{1}{RT}\int_{\infty}^{V}(\frac{RT}{V} - P)dV - 1 - Inz \tag{19}$$

Equation (19) is transformed to Equation (20),

$$In(\frac{f}{RT}) + Inb = \frac{PV}{RT} - In\frac{V-b}{b} - \frac{a}{bRT}In\frac{V+b}{V} - 1 \tag{20}$$

Let $\alpha = \frac{a}{bRT}$, $u = \frac{V}{b}$, the simplified equation for calculating the fugacity factor of a mixture using zero pressure as the reference state can be given in Equation (21).

$$In\frac{f_0}{RT} + Inb = -1 - \alpha In\frac{u+1}{u} - In(u-1) = Q(u,\alpha) \tag{21}$$

Solve for the minimum root u:

$$\frac{Pb}{RT} = \frac{1}{u-1} - \frac{\alpha}{u(u+1)} = 0 \tag{22}$$

$$u = 0.5 \times \left[(\alpha - 1) - (\alpha^2 - 6\alpha + 1)^{0.5}\right] \tag{23}$$

Combining Equation (23) with Equation (21) yields Equation (24).

$$Inb + In\frac{f_0}{RT} = Q[u(\alpha), a] = q(\alpha) \tag{24}$$

For pure substances,

$$Inb_{ii} + In\frac{f_{i,0}}{RT} = q(\alpha_{ii}) \tag{25}$$

The equation for the SRK equation to calculate G^E is Equation (26):

$$\left(\frac{G^E}{RT}\right)^{EoS} = \sum_i x_i In\frac{f_{i,0}}{RT} + In\frac{f_0}{RT} \tag{26}$$

that is,

$$\sum_i x_i In\frac{b}{b_{ii}} + \sum_i x_i q(\alpha_{ii}) + \left(\frac{G^E}{RT}\right)^{EoS} = q(\alpha) \tag{27}$$

let $q(\alpha) \approx q_0 + q_1\alpha$,

$$q(\alpha) - \sum_i q(\alpha_{ii})x_i \approx q_1\alpha - q_1\sum_i \alpha_{ii}x_i \tag{28}$$

Combining Equations (21) and (27), the G^E mixing rule Equation (29) based on elements and chemical bonds can be derived.

$$\alpha = \frac{1}{q_1}\left[\frac{G^E}{RT} + \sum_i x_i In(\frac{b}{b_{ii}})\right] + \sum_i x_i\alpha_{ii} \tag{29}$$

For the mixture, the parameter b can be calculated from the following Equation (30).

$$b = \sum_i b_i x_i \tag{30}$$

The UNICAC model is used to calculate the G^E in Equation (29). The SRK equation, Equations (29) and (30) then form a completely new element- and chemical bond-based G^E-EoS model, called the SRK-UNICAC model.

2.2.5. Parameters Determination

The G^E-EoS model draws on the advantages of the equation of state and activity coefficient methods. In fact, it is also inevitably subject to the limitations of the equation of state and activity coefficient models themselves. Many existing G^E-EoS models are proposed based on UNIFAC and its modified models. Although the parameters of UNIFAC and its modified models have been revised and extended several times, a complete set of parameters has not been proposed so far. The UNICAC model reduces the basic contribution unit by changing the group division, which greatly reduces the possibility of missing group-interaction parameters and well compensates for the deficiency of the UNIFAC model.

In the SRK-UNICAC model-building process, some assumptions and formulae simplifications were used. Simultaneously, some optimization algorithms [18] were used to enhance the regression-fitting process of the equations. The details are described as follows.

(1) The assumption that the reference state pressure is zero is used in the model.

(2) Let $q(\alpha) \approx q_0 + q_1\alpha$. Different scholars take different values for 1 in the MHV1 model [11,12]. According to Holderbaum's proposal, $q_1 = -0.64663$.

(3) The group-interaction parameters already fitted by the UNICAC model [14] were used, and the G^E was calculated based on this model.

(4) The component-related parameters C_1, C_2, and C_3 were taken from reference [19]. The critical thermodynamic properties of organic compounds are derived from reliable experimental data or using relevant predictive models of accurate thermodynamic properties [20].

2.2.6. Comparison of Different Mixing Rules

Most of the mixing rules are empirical. Different mixing rules or different values of mixing parameters within the same mixing rule tend to be sensitive to the computational results. This is especially true for systems with widely varying properties. Since the EoS method is very dependent on the mixing rules, different forms of fugacity coefficient formulas can be derived from using different mixing rules in EoS. The appropriate use of mixing rules directly affects the effectiveness of the fugacity coefficient in phase equilibrium calculations.

When the EoS method is used for the phase equilibrium calculation of a mixture, the corresponding mixing rules must be used. The SRK-UNICAC model combines EoS and excess Gibbs function to obtain a new mixing rule(SRK-UNICAC).

Table 1 shows the difference between the SRK-UNICAC model and other G^E mixing rules.

Table 1. The comparison of different mixing rules.

G^E Mixing Rules	EoS	Activity Coefficient Model	Reference State Pressure
HV	RK	NRTL	infinite
MHV1/MHV2	SRK	Wilson	0
PSRK	SRK	UNIFAC	0
WS	PR	NRTL	infinite
LCVM	PR	UNIFAC	no definite
SRK-UNICAC	SRK	UNICAC	0

As can be seen in Table 1, the current classical G^E mixing rules usually use SRK, RK, and PR cubic equations of state. Zero pressure, infinite pressure, or no definite pressure is chosen as the reference state in the derivation process. It also uses activity factor models such as NRTL, Wilson, and UNIFAC. When zero pressure is the reference state, the SRK equation of state is generally chosen. Therefore, SRK-UNICAC is no exception and can follow the interaction parameters of the original activity coefficient model.

3. Model Assessment

3.1. Evaluation Method

The bubble-point calculation method is used to predict the VLE of a mixture by an iterative approach. The bubble-point computational method is divided into two types. One is the bubble-point temperature and vapor phase composition calculation, and the other is the bubble-point pressure and vapor phase composition calculation. Figure 2 shows an example of the first bubble-point calculation process with the help of Matlab software.

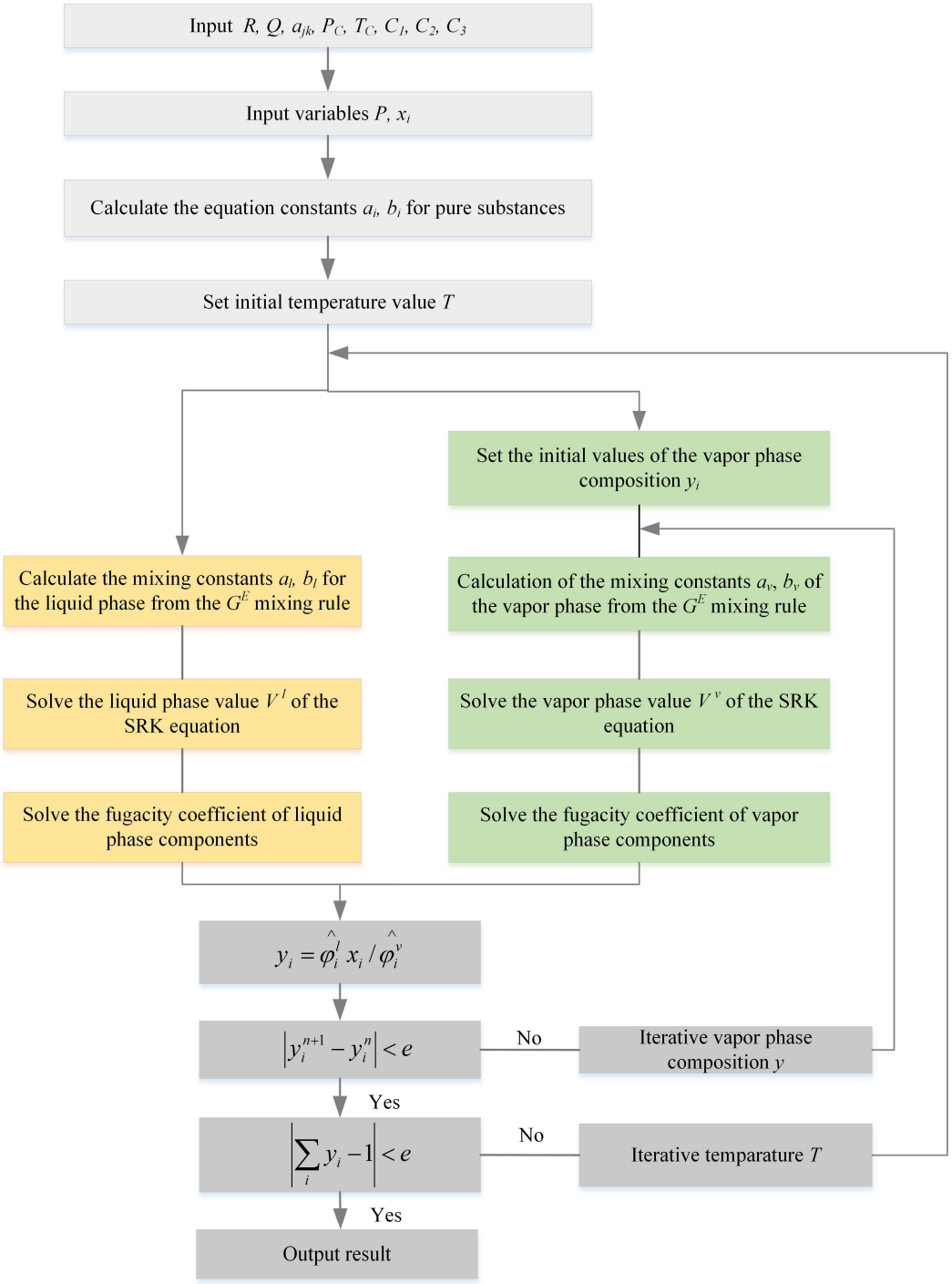

Figure 2. Block diagram of the calculation of bubble-point temperature and vapor phase composition.

In order to ensure that the program converges more easily, the convergence accuracy of the set algorithm should not be too small. Therefore, the convergence accuracy is set to 10^{-4},

while the initial value of the iteration is selected as the temperature of the experimental data. The iterative calculation of the vapor phase composition was performed using the natural iteration method, and the temperature T was calculated using Equation (31):

$$T = T + 0.1 \times T(1 - \sum_i y_i) \tag{31}$$

Equally, by replacing the temperature T in block diagram Figure 2 with the pressure P for iteration, the bubble-point pressure can be calculated. The P is obtained through an iterative calculation with Equation (32).

$$P^{n+1} = P^n \sum_{i=1}^{N} y_i^n \tag{32}$$

3.2. Prediction Results of Binary Systems under Low and Medium Pressure Conditions

To evaluate the SRK-UNICAC model, 87 sets of experimental data on VLE of binary systems under low- and medium-pressure conditions were selected from references [21–28]. It should be indicated that none of these data are involved in the fitting process of the group-interaction parameters of the UNICAC model. To ensure the accuracy of the evaluation results, the above binary systems cover a wide range of compounds. It also includes 43 elements and chemical bonds, such as C, H, N, Si, S, O, C-H, O-H, C=O, etc., which are required for the composition of compounds.

Five activity coefficient models were selected: UNICAC, UNIFAC(Dortmund) [29], UNIFAC(Lyngby) [30], UNIFAC(2003) [31], and ASOG(2011) [32]. These models were analyzed and compared with the SRK-UNICAC model. The prediction date of the above five models was obtained from Xia(2022) [14]. The vapor–liquid equilibrium results for the 87 groups of binary systems under low- and medium-pressure conditions predicted by the SRK-UNICAC model are shown in Table A1.

According to Table A1, the SRK-UNICAC model was able to successfully predict 89.7% of the total evaluated systems. A total of nine groups of binary systems, such as methanol + 2,3-dimethoxy-1-propanol, tert-butanol + water, vinyl acetate + ethyl butyrate, cannot be predicted. The main reason is that SRK-UNICAC lacks the component-related parameters C_1, C_2, and C_3.

3.3. Prediction Results of Binary System under High-Pressure Conditions

In order to compare the predictive capability and application of the SRK-UNICAC model under high-pressure conditions, VLE predictions were performed using five other models for 12 groups of binary systems.

The temperature, pressure, and vapor phase composition of the VLE of a 12-group binary system at high pressure were calculated using the SRK-UNICAC model. All data are shown in Table 2. The prediction results and error analysis for the other five groups of contributing activity coefficient models are shown in Table 3.

Table 2. Comparison of VLE of binary system predicted by SRK-UNICAC model under high pressure with experimental data.

NO.	System	T, K	P, kPa	N	MAEy	MAEP or MAET	MREy, %	MREP or MRET, %
1	isoprene + acetonitrile	342.92–381.30	309.06	19	0.0126	0.00 K	2.14	0.00
2	2-methyl-2-butene + acetonitrile	344.92–368.36	300.95	16	0.0423	1.32 K	6.09	0.37
3	acetonitrile + water	385.16–385.66	300.95	8	0.0451	9.01 K	7.70	2.34
4	water + ethylenediamine	422.64–436.58	369.85	10	0.0643	23.27 K	12.80	5.40
5	1-butene + 1,3-butadiene	310.93	416.52–430.12	9	0.0118	0.10 kPa	3.61	1.17
6	1-butene + n-butane	310.93	364.66–425.59	9	0.0056	4.61 kPa	0.96	1.16
7	ethane + n-butane	338.71	3543.90–5550.20	6	0.0143	2.00 kPa	1.75	3.82
8	ethane + n-butane	366.48	3709.40–5481.30	8	0.0302	0.31 kPa	6.43	0.72
9	ethane + diethyl ether	298.15	9559.00–3856.70	6	0.0049	1.93 kPa	0.50	8.39
10	ethane + propionic acid	298.15	480.50–3651.00	9	0.0245	7.66 kPa	2.50	31.27
11	ethane + benzene	298.15	775.90–3800.60	7	0.0015	3.65 kPa	0.15	17.02
12	ethane + n-hexane	298.15	507.80–3549.40	7	0.0040	1.86 kPa	0.41	7.24

Table 3. The other five models predict the VLE of the binary system at high pressure in comparison with experimental data.

NO.	System	UNICAC		UNIFAC (2003)		UNIFAC (Dortmund)		UNIFAC (Lyngby)		ASOG (2011)	
		MREP or MRET, %	MREy, %	MREP or MRET, %	MREy, %	MREP or MRET, %	MREy, %	MREP or MRET, %	MREy, %	MREP or MRET, %	MREy, %
1	isoprene + acetonitrile	0.31	6.23	0.32	6.31	0.46	7.73	-	-	0.51	3.52
2	2-methyl-2-butene + acetonitrile	0.63	2.31	1.25	6.88	0.49	2.61	-	-	0.19	1.36
3	acetonitrile + water	3.61	16.21	0.52	2.94	0.28	1.64	-	-	0.40	2.48
4	water + ethylenediamine	4.84	30.70	0.31	1.35	-	-	-	-	0.68	12.41
5	1-butene + 1,3-butadiene	1.28	2.39	1.07	2.32	0.76	1.99	0.62	1.61	0.86	1.22
6	1-butene + n-butane	0.90	1.65	1.40	2.02	1.16	1.84	0.46	1.33	1.08	1.69
7	ethane + n-butane	20.83	11.92	27.07	13.75	33.31	13.72	28.70	11.91	24.17	13.76
8	ethane + n-butane	33.31	26.34	43.68	37.12	55.45	38.33	46.91	27.17	38.31	36.51
9	ethane + diethyl ether	13.47	2.13	25.04	2.35	23.36	2.33	14.10	2.14	4.36	1.86
10	ethane + propionic acid	64.97	2.42	95.51	2.59	111.47	2.60	94.90	2.50	66.78	2.48
11	ethane + benzene	28.01	0.57	10.04	0.50	16.58	0.63	11.57	0.48	23.59	0.48
12	ethane + n-hexane	11.52	0.81	6.81	1.07	26.17	1.27	13.11	1.14	6.87	0.96

Note: '-' means that the vapor-liquid phase balance of this system cannot be predicted by the model.

3.4. Prediction Results of Ternary System under Low and Medium Pressure Conditions

The VLE behavior of 14 sets of ternary systems under low- and medium-pressure conditions was predicted with the SRK-UNICAC model and five other activity coefficient models. Experimental data were obtained from reference [21]. The errors in P or T and y for the other five models predicting the VLE for the selected ternary system were taken from Xia(2022) [14]. The predictive ability of the SRK-UNICAC model in predicting the VLE of ternary systems under low- and medium-pressure conditions was examined by analyzing and comparing the prediction results. The predictions of the SRK-UNICAC model for predicting the VLE of the ternary system under low- and medium-pressure conditions are shown in Table 4. Table 4 indicates that for the VLE of the ternary system, the new model predicts the vapor-phase fraction more accurately. The mean absolute error of the vapor-phase fractions y_1, and y_2 are within 0.03 for 96.43% of the ternary systems.

Table 4. Comparison of VLE of ternary systems predicted by the SRK-UNICAC model under low- and medium-pressure conditions with experimental data.

NO.	System	Data Type P or T	N	$MAEy_1$	$MAEy_2$	MAET or MAEP	$MREy_1$- %	$MREy_2$ %	MRET or MREP %
1	acetone + methanol + ethanol	101.33 kPa	83	0.1251	0.0105	0.6388 K	7.86	3.37	0.19
2	methanol + ethanol + 1-propanol	101.33 kPa	45	0.0158	0.0106	0.8198 K	5.41	3.52	0.23
3	acetone + methanol + 2-propanol	328.15 K	27	0.0122	0.0089	1.3739 kPa	6.89	3.25	2.04
4	2,3-dimethylbutane + methanol + acetone	101.33 kPa	27	0.0284	0.0248	3.1841 K	7.68	8.88	1.00
5	methanol + 2-methylbutane + isoprene	101.33 kPa	13	0.0267	0.0171	0.7532 K	26.47	3.89	0.25
6	methanol + heptane + toluene	101.33 kPa	8	0.0106	0.0123	1.4424 K	1.37	9.11	0.43
7	acetone + ethanol + hexane	328.15 K	21	0.0173	0.0102	13.559 kPa	4.55	5.19	12.79
8	hexane + ethanol + benzene	328.15 K	43	0.0163	0.0208	6.1478 kPa	5.32	6.52	7.87
9	ethanol + benzene + heptane	53.33 kPa	50	0.0176	0.0157	1.3968 K	4.63	4.92	0.43
10	ethanol + benzene + heptane	101.33 kPa	47	0.0219	0.0128	1.9993 K	4.95	5.15	0.58
11	benzene + heptane + 1-propanol	348.15 K	77	0.0199	0.0104	3.8307 kPa	5.72	4.2	4.67
12	acetone + 2-methylbutane + isoprene	101.33 kPa	15	0.0096	0.0156	2.0886 K	4.54	3.23	0.69
13	butanone + 3-pentanone + 4-methyl-2-pentanone	101.33 kPa	64	0.0112	0.0045	0.4001 K	2.95	2.31	0.11
14	2-butanol + sec-butyl acetate + N,N-dimethylacetamide	101.33 kPa	14	0.0091	0.0138	2.1602 K	2.76	3.10	0.54

4. Results and Discussion

4.1. Comparison and Analysis of Binary System Results under Low- and Medium-Pressure Conditions

Four binary systems were randomly selected, and the VLE results of the binary systems predicted with six different models were compared with the experimental data. The *x-y* and *x-P* plots were then plotted; see Figures 3–6. Thus, the predictive ability of different models can be evaluated more visually.

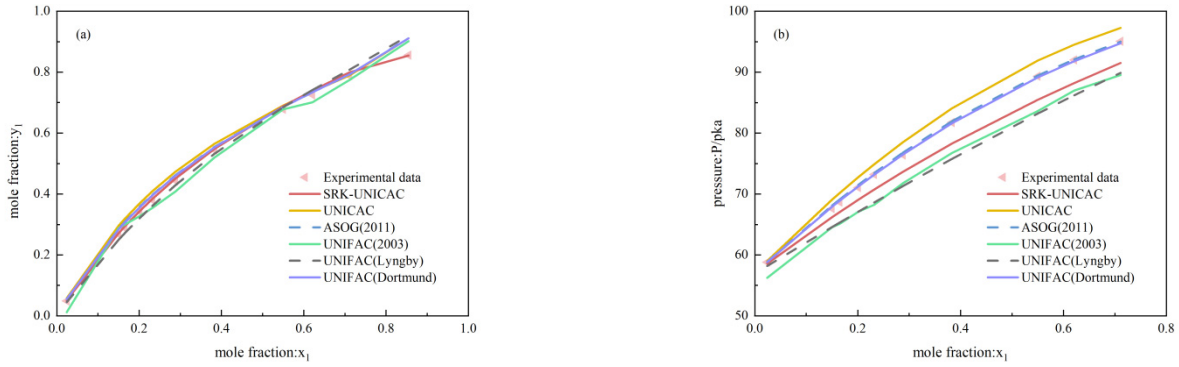

Figure 3. Comparison of the predictive power of different models for the VLE behavior in the benzene + heptane system. Figure (**a**) shows the *x-y* figure for the benzene + heptane system and figure (**b**) shows the *x-P* figure for the benzene + heptane system.

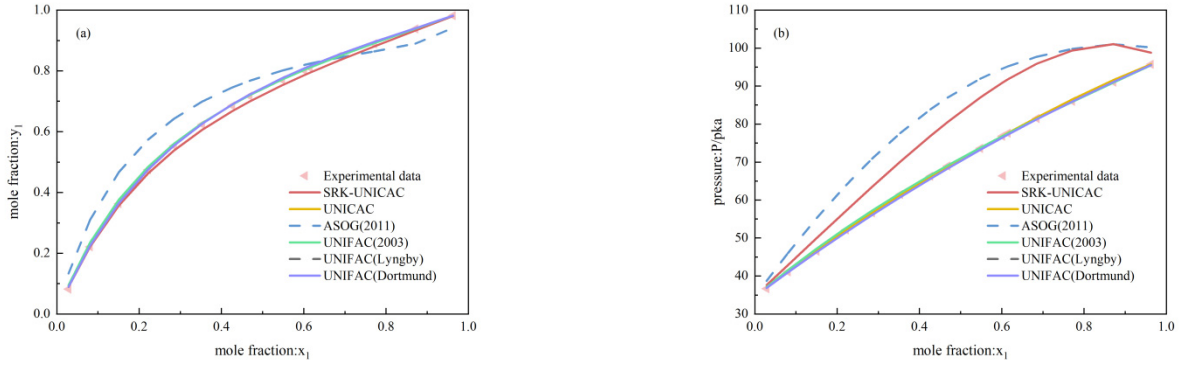

Figure 4. Comparison of the predictive power of different models for the VLE behavior in the carbon disulfide + carbon tetrachloride system. (**a**) shows the *x-y* figure for the carbon disulfide + carbon tetrachloride system and figure (**b**) shows the *x-P* figure for the carbon disulfide + carbon tetrachloride system.

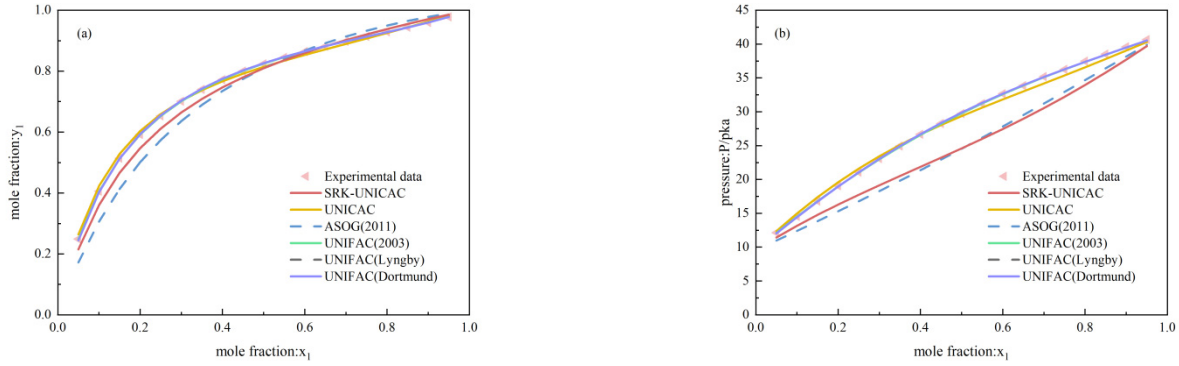

Figure 5. Comparison of the predictive power of different models for the VLE behavior in the carbon tetrachloride + pyridine system. (**a**) shows the *x-y* figure for the carbon tetrachloride + pyridine system and figure (**b**) shows the *x-P* figure for the carbon tetrachloride + pyridine system.

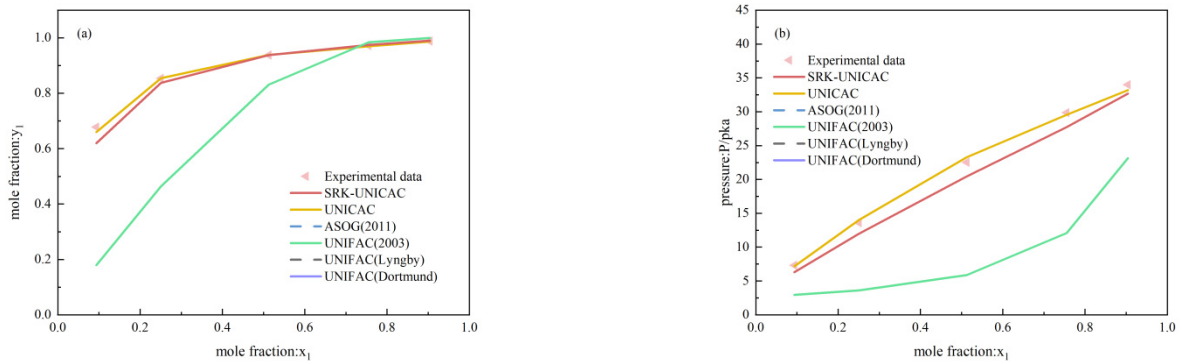

Figure 6. Comparison of the predictive power of different models for the VLE behavior in the benzene + tetraethyl silicane system. (**a**) shows the *x-y* figure for the benzene + tetraethyl silicane system and figure (**b**) shows the *x-P* figure for the benzene + tetraethyl silicane system.

It is evident from Figure 3 that all six models can predict the vapor phase composition of the benzene + heptane system with good prediction accuracy. With regards to the bubble-point pressure of this system, UNIFAC(2003) and UNIFAC(Lyngby) have a large error in predicting it, and the degree of deviation of the predicted values from the experimental values can be clearly seen in Figure 3. The prediction ability of SRK-UNICAC in this respect is comparable to UNICAC and slightly better than the two models UNIFAC(2003) and UNIFAC(Lyngby).

From Figures 4 and 5, the SRK-UNICAC model can predict the vapor phase composition of the carbon disulfide + carbon tetrachloride system and the carbon tetrachloride + pyridine system very well and with high accuracy. As a matter of fact, the SRK-UNICAC model's error in predicting the bubble-point pressure is slightly larger and only slightly better than that of the ASOG model, which has a larger error in predicting the VLE for the above two systems. The other four models have higher accuracy for prediction.

For the benzene + tetraethyl silicane system, only three models possess the predictive capability for this system, as shown in Figure 6. Among them, the SRK-UNICAC and UNICAC models can predict the VLE behavior of this system with high accuracy, and the predicted points are in high agreement with the experimental points. UNIFAC (2003) predicts unsatisfactory results with large errors. The other three models do not have the ability to predict the VLE of the benzene + tetraethyl silicane system.

Analyzing Figures 3–6, the accuracy of the SRK-UNICAC model in predicting the bubble pressure for the binary system is less than satisfactory at bubble-point pressures below 1 atm. However, it is obvious that the SRK-UNICAC model is fully capable of predicting the vapor phase composition of systems containing polar and nonpolar substances with high accuracy. In the meantime, the prediction range is broadened, and it can effectively predict a benzene + tetraethyl silicane system that cannot be predicted by most models. Since ASOG(2011), UNIFAC(Dortmund), and UNIFAC(Lyngby) do not have silicon-containing groups and cannot predict systems containing silicon compounds, only SRK-UNICAC, UNICAC, and UNIFAC(2003) can predict with high prediction accuracy. UNIFAC(2003) can only predict a small number of silicon-containing systems because of the fine group division, and the prediction range is not comprehensive.

VLE predictions were performed using six models for 87 groups of binary systems under low- and medium-pressure conditions. The prediction ranges, vapor phase composition, temperature, and pressure predictions for each model are presented in Table 5.

Table 5. Comparison of the predictive ability of the six models for the VLE of the binary system under low- and medium-pressure conditions.

Model	N	MREP or MRET %	MREy %
SRK-UNICAC	78	9.61	8.68
UNICAC	87	3.63	7.46
UNIFAC(2003)	75	7.30	10.87
UNIFAC(Dortmund)	67	3.24	5.53
UNIFAC(Lyngby)	44	9.81	9.66
ASOG(2011)	73	7.84	12.28

Due to the absence of group-interaction parameters, the VLE of some systems cannot be predicted by the UNIFAC model due to missing parameters, which largely limits the scope of application of the UNIFAC model. The element- and chemical bond-based activity coefficient model(UNICAC model) reduces the basic contribution units by changing the group division, which greatly reduces the possibility of missing group-interaction parameters and compensates well for the deficiencies of the UNIFAC model.

As can be seen from Table 5, due to the use of elements and chemical bonds groups to split the molecular structure, almost all of the complex organic substances that currently occur in the chemical industry can be split in this way. By combining with the UNICAC model, the SRK-UNICAC model makes up for a large number of group-interaction parameters in the UNIFAC model, thus enabling a wider prediction range. The SRK-UNICAC model and the UNICAC model are therefore able to predict a wider range of substances than other models. The SRK-UNICAC model outperforms the UNIFAC(2003), UNIFAC(Lyngby), and ASOG(2011) models in predicting the vapor phase molar fraction for binary systems under low- and medium-pressure conditions. The SRK-UNICAC model also predicts the temperature of the binary system under low- and medium-pressure conditions with slightly better pressure accuracy than the UNIFAC model. The new activity coefficient model can therefore allow prediction of the VLE under low- and medium-pressure conditions and can meet a certain level of scientific research needs.

4.2. Comparison and Analysis of Binary Systems Results under High-Pressure Conditions

The results of the comparison between the predicted data of the SRK-UNICAC model and the other five models for the VLE of the binary system under high pressure and the experimental data are listed in Table 6.

Table 6. Comparison of the predictive ability of the six models for the VLE of the binary system under high-pressure conditions.

Model	MAEy	MREP or MRET %	MREy %
SRK-UNICAC	0.0217	6.58	3.75
UNICAC	0.0588	15.31	8.64
UNIFAC(2003)	0.0436	17.75	6.60
UNIFAC(Dortmund)	0.0456	24.50	6.79
UNIFAC(Lyngby)	0.0530	26.30	6.03
ASOG(2011)	0.0408	13.98	6.56

Although the activity coefficient model predicts the VLE well under low- and medium-pressure conditions, it tends to have large prediction errors under high-pressure conditions. The main reason for this is that the non-ideal nature of the vapor phase under high-pressure conditions is becoming increasingly apparent. Therefore, the SRK-UNICAC model, which incorporates a cubic equation of state, can predict the VLE under high-pressure conditions more accurately. As shown in Table 6, the mean relative error of the SRK-UNICAC model for the vapor-phase fraction and bubble-point pressure for the high-pressure binary system

is 3.75% and the mean relative error for temperature is 6.58%, respectively. The prediction accuracy is much higher than in the other five models, especially significantly higher than the 15.31% and 8.64% of UNICAC. This indicates that the element- and chemical bond-based G^E-EoS model(SRK-UNICAC) has been successfully extended to high-pressure polar systems. The improvement of the element- and chemical bond-based activity coefficient model UNICAC is significant.

4.3. Comparison and Analysis of Ternary Systems Results under Low- and Medium-Pressure Conditions

The SRK-UNICAC model's detailed predictions for the VLE of the ternary system under low- and medium-pressure conditions are listed in Table 4. Figure 7a–j shows the predicted data of vapor-phase fraction for some ternary systems compared with the experimental data. The horizontal and vertical coordinates indicate the experimental and predicted values of the vapor phase molar fraction, respectively. The closer the data points are to the function $y = x$, the better the predicted vapor phase molar fraction matches the experimental value and the higher the prediction accuracy of the model.

It is obvious from Figure 7a–j that the vast majority of data points with experimental data as horizontal coordinates and predicted data as vertical coordinates are distributed on the function $y = x$. The R^2 was calculated for the predicted results of 14 groups of ternary systems with experimental values, and it was found that 90.48% of the R^2 reached above 0.96. The results show that the estimated data of the SRK-UNICAC model for the ternary system under low- and medium-pressure conditions have small errors with the experimental data, which proves the satisfactory predictive ability of the new model.

The VLE of the ternary system was predicted using the SRK-UNICAC model and five other models. The calculated vapor-phase fractions, temperatures, and pressures for all systems were treated as average absolute deviations from the experimental values. The specific results are listed in Table 7. Table 7 indicates that the mean relative errors of the SRK-UNICAC model for the vapor-phase fraction y of component 1 and component 2 are 6.50% and 4.76%, respectively, which are better than almost all models. Meanwhile, the model is also more accurate for the prediction of pressure or temperature, with a mean relative error of 2.52%, which can satisfy the scientific research needs to a certain extent, although it is slightly higher than the other models. Therefore, it is generally seen that the SRK-UNICAC model is outstanding in predicting the VLE of ternary systems.

Table 7. Comparison of the predictive ability of the six models for the VLE of the ternary system under low- and medium-pressure conditions.

Model	$MREy_1$ %	$MREy_2$ %	MREP or MRET %
SRK-UNICAC	6.50	4.76	2.25
UNICAC	10.91	6.95	1.37
UNIFAC(2003)	8.38	6.64	0.82
UNIFAC (Dortmund)	7.39	4.35	0.66
UNIFAC(Lyngby)	8.05	5.30	0.89
ASOG(2011)	7.40	4.86	0.89

The analysis of the above results demonstrates that the development of the SRK-UNICAC model is relatively successful and has a high predictive capability, especially for binary systems containing polar components under high pressure and ternary systems under low- and medium-pressure conditions. At the same time, it can accurately predict the VLE of low- and medium-pressure binary systems. The SRK-UNICAC model further contributes to solving the problem of predicting the accuracy and range of VLE of mixtures.

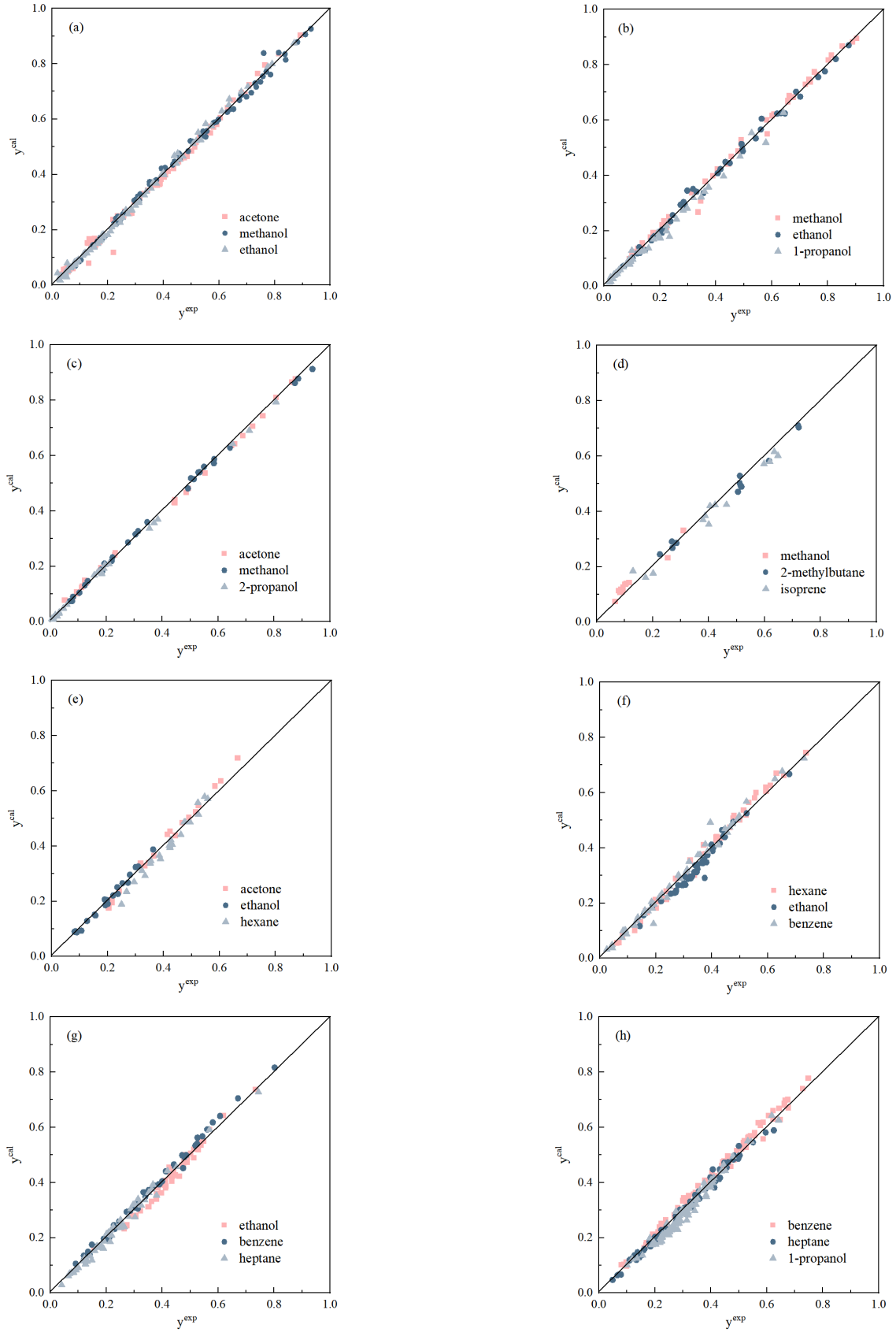

Figure 7. *Cont.*

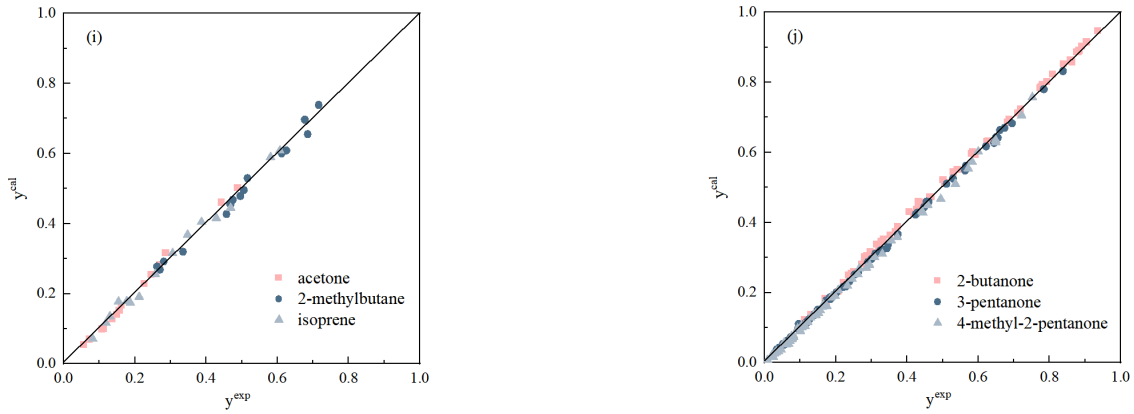

Figure 7. Comparison of VLE prediction data of SRK-UNICAC model for different ternary systems under low- and medium-pressure conditions with experimental data (**a**–**j**).

5. Conclusions

By choosing zero pressure as the reference state pressure, a new G^E-EoS model(SRK-UNICAC) was developed by combining the UNICAC activity coefficient model and the SRK cubic equation of state. The new model and five other activity coefficient models were applied to predict the VLE of binary and ternary systems under different pressures. Although the SRK-UNICAC model differs somewhat from experimental data in predicting bubble-point pressures below 1 atm, the SRK-UNICAC model predicts VLE for binary systems containing nonpolar and polar compounds under low- and medium-pressure conditions better than UNIFAC(Lyngby), UNIFAC(2003), and ASOG(2011). Additionally, the SRK-UNICAC model is much more accurate than all the other five models for binary systems containing polar components under high pressure and also has a more accurate prediction of the vapor-phase fraction for ternary systems containing both polar and nonpolar substances. It is worth mentioning that the new model has also made some progress in expanding the prediction range.

Author Contributions: Formal analysis, Investigation, B.N. and W.M.; Conceptualization, Methodology, Software, Writing—review and editing, X.S. and L.X.; Formal analysis, Validation, Visualization, Writing—original draft, X.L.; Resources, Supervision, Validation, Project administration, W.Z. and S.X. All authors have read and agreed to the published version of the manuscript.

Funding: This work was supported by the National Natural Science Foundation of China (NO. 22178190, Shuguang Xiang) and the National Youth Natural Science Foundation of China (NO. 22008129, Wenying Zhao).

Data Availability Statement: The data presented in this study are available from the corresponding author upon request.

Conflicts of Interest: The authors declare no conflict of interest.

Nomenclature

A^E	Excess Helmholtz free energy, $J \cdot mol^{-1}$
A_k	Surface area of group k, $m^2 \cdot mol^{-1}$
MAEP	Mean absolute error in bubble-point pressure, kPa
MAET	Mean absolute error in bubble-point temperature, K
MAEy	Mean absolute error in vapor-phase fraction
$MAEy_1$	Mean absolute error in the vapor-phase fraction of component 1
$MAEy_2$	Mean absolute error in the vapor-phase fraction of component 2
MRET	Mean relative error in vapor-phase fraction, %
MREP	Mean relative error in bubble-point pressure, %
MREy	Mean relative error in vapor-phase fraction, %

$MREy_1$	Mean relative error in the vapor-phase fraction of component 1, %
$MREy_2$	Mean relative error in the vapor-phase fraction of component 2, %
a	Activity
a_i	Energy parameters of state equation for pure components, $kPa \cdot m^6 \cdot K^{0.5} \cdot mol^{-2}$
a_{kl}	Interaction parameters of the UNICAC model for group interactions, K
B_{ij}	Binary cross-variance factor, $m^3 \cdot mol^{-1}$
b	Co-Volume parameters for mixtures of the equation of state, $m^3 \cdot mol^{-1}$
C_1,C_2,C_3	Component-dependent parameters in the SRK equation
f	Fugacity, kPa
G^E	Excess Gibbs free energy, $J \cdot mol^{-1}$
k_{ij}	Binary interaction parameter with a magnitude of 1
M	Activity coefficient model
N	Number of data points
P	Total pressure of the system, kPa
P_c	Critical pressure, kPa
Q_k	Surface area parameters of the elements and chemical bonds
q	Molecular surface area parameters
q_0	Model parameters for MHV1 and PSRK mixing rules
q_1	Model parameters for the MHV2 mixing rule
R	Gas constants, 8.314 $J \cdot mol^{-1} \cdot K^{-1}$
R_k	Volume parameters of the elements and chemical bonds
r	Molecular volume parameters
T	Temperature, K
T_c	Critical temperature, K
T_r	Reference temperature
V	Molar volume of the mixture, $m^3 \cdot mol^{-1}$
V_i	Molar volume of pure substance, $m^3 \cdot mol^{-1}$
V_k	Volume of group *k*, $m^3 \cdot mol^{-1}$
$V_k^{(i)}$	The number of elements and bonds in the molecule
X_i	The fraction of elements and chemical bonds of l in liquid solution
x	Liquid phase molar fraction
y	Vapor phase molar fraction
Γ_k	Group activity coefficient
θ	Volume fraction
Φ	Area fraction
φ	Fugacity coefficient
γ	Activity coefficient

Appendix A

Table A1. Comparison of VLE of binary systems predicted by SRK-UNICAC model with experimental data under low- and medium-pressure conditions.

No.	System	P or T	N	MAET or MAEP	MREP or MRET %	MAEy	MREy %
1	water + phenol		12	22.99 K	6.28	0.4096	44.3
2	benzene + isopropanol	66.66 kPa	14	0.00 K	0	0.0185	5.49
3	ethyl formate + cyclohexane		9	0.07 K	22.59	0.2083	0.12
4	methyl formate + N,N-dimethylformamide	74.66 kPa	15	0.00 K	0	0.0548	0.04
5	trichloroethylene + acetic acid	93.33 kPa	9	2.74 K	0.75	0.0727	11.03
6	trichlorosilane + silicon tetrachloride	98.70 kPa	11	0.00 K	0	0.0099	24.97
7	ether + Dichloromethane	99.02 kPa	27	0.00 K	0	0.013	7.11
8	methanol + 1,2-ethanediol		12	9.01 K	2.41	0.0646	12.56
9	ethanol + 2-methyl-1-propanol		14	0.00 K	0	0.0159	2.53
10	toluene + 3-methyl-1-butanol		15	0.34 K	34	0.1583	15.83

Table A1. *Cont.*

No.	System	P or T	N	MAET or MAEP	MREP or MRET %	MAEy	MREy %
11	benzene + 2-methyl-1-propanol		31	1.24 K	0.35	0.0533	8.14
12	methanol + epichlorohydrin		10	0.00 K	0.22	0.0548	8.01
13	methanol + 2,3-dimethoxy-1-propanol		19	-	-	-	-
14	ethanol + water		20	0.00 K	1.91	0.0264	36.6
15	ethanol + tert-butanol		18	0.00 K	0.14	0.0557	5.57
16	tert-butanol + ethyl tert-butyl ether		18	0.00 K	0.09	0.1004	10.04
17	ethyl tert-butyl ether + ethanol		18	0.00 K	0	0.0957	9.57
18	tert-butanol + water		18	-	-	-	-
19	methyl formate + dimethanol acetal		14	0.00 K	0	0.0775	7.75
20	methyl formate + dimethyl carbonate		14	0.00 K	0	0.0546	5.46
21	dimethyl acetal + dimethyl carbonate		14	0.00 K	0.07	0.1229	12.29
22	methanol + epichlorohydrin		10	0.00 K	0.22	0.0803	8.03
23	methanol + 2,3-dimethoxy-1-propanol		19	-	-	-	-
24	acetic acid + pentyl acetate		14	0.60 K	0.15	0.0955	16.27
25	methanol + ethyl butyrate		19	0.69 K	0.2	0.0746	9.7
26	vinyl acetate + ethyl butyrate		19	-	-	-	-
27	chlorodifluoromethane + ethanol		4	40.11 K	13.52	0.5628	4.69
28	chlorodifluoromethane + propanol		4	56.01 K	18.68	0.7172	0.78
29	difluoromethane + methanol		4	34.31 K	11.64	0.6099	5.74
30	difluoromethane + ethanol		4	47.76 K	16.17	0.7272	9.16
31	1,1-difluoroethane + methanol		4	36.92 K	12.53	0.6984	4.62
32	difluoromethane + isopropanol		4	14.89 K	5.3	0.8338	10.04
33	1,1-difluoroethane + ethanol		4	28.18 K	9.69	0.8448	3.07
34	1,1-difluoroethane + isopropanol		4	59.32 K	20.25	0.9127	4.8
35	isopropyl alcohol + water		8	0.85 K	3.06	0.1925	34.34
36	2-butanol + water		17	13.89 K	3.84	0.1827	35.24
37	chloroform + ethanol		16	0.00 K	0	0.0436	10.77
38	cyclohexane + isobutanol		12	0.00 K	0	0.0234	4.25
39	acetone + propyl acetate		15	0.00 K	0	0.0304	5.98
40	methyl acetate + benzene		12	0.00 K	0	0.0264	0.01
41	methylcyclopentane + benzene		35	0.00 K	0	0.0344	0.01
42	benzene + methylcyclohexane		25	0.00 K	0	0.0526	0.03
43	1—chloropropane + methanol	101.60 kPa	10	0.00 K	0	0.0448	6.11
44	benzene + butanol	192.66 kPa	10	2.85 K	0.72	0.0698	13.52
45	dichlorosilane + trichlorosilane	700.00 kPa	6	-	-	-	-
46	dichlorosilane + trichlorosilane	1400.00 kPa	6	-	-	-	-
47	dichlorosilane + trichlorosilane	2100.00 kPa	6	-	-	-	-
48	monochlorodifluoromethane + dichlorodifluoromethane	223.15 K	16	0.14 kPa	8.09	0.127	0.06
49	benzene + anthranilic acid	298.15 K	18	4.45 kPa	33.63	0.234	44.35
50	hexane + benzene		12	0.06 kPa	1.06	0.0436	0.02
51	acetone + vinyl acetate		11	2.11 kPa	6.42	0.0183	4.92
52	acetone + tetraethylsilane	308.15 K	9	12.64 kPa	46.13	0.0692	7.6
53	carbon disulfide + tetrachloroethylene		12	0.14 kPa	6.73	0.0219	0.02
54	dimethoxymethane + carbon disulfide	308.32 K	36	4.68 kPa	5.23	0.0263	6.22
55	ethanol + 1,2-dichloroethane	313.15 K	10	-	-	-	-
56	acetone + benzene		11	0.10 kPa	9.98	0.065	6.5
57	ethyl formate + chloroform		10	0.03 kPa	1.7	0.1379	0.03
58	perfluorohexane + hexane	318.15 K	17	0.45 kPa	39.01	0.3346	0.18
59	carbon disulfide + carbon tetrachloride		15	0.12 kPa	8.76	0.0215	0.01
60	chloroform + dimethyl sulfoxide		14	0.93 kPa	16.19	0.0291	0.02
61	benzene + acetic acid	323.14 K	10	0.29 kPa	8.1	0.1162	0.03
62	hexane + 1-pentanol		13	0.35 kPa	34.81	0.0748	7.48
63	toluene + 4-methyl-2-pentanone		26	0.00 kPa	0.32	0.016	1.6
64	ethyl iodide + heptane	323.15 K	18	0.05 kPa	1.73	0.034	0.02
65	benzene + tetraethylsilane		7	0.09 kPa	1.63	0.0219	0.02
66	carbon tetrachloride + pyridine		21	0.13 kPa	3.51	0.038	0.02
67	ethyl acetate + propionic acid		9	0.52 kPa	4.54	0.0414	11.41
68	butyraldehyde + acetic acid	323.20 K	9	5.41 kPa	21.52	0.0093	2.43
69	methyl ethyl ketone + propionic acid		9	-	-	-	-
70	acetone + methanol		11	0.02 kPa	1.87	0.0354	3.54
71	ethyl acetate + ethanol	328.15 K	14	4.00 kPa	7.92	0.0329	10.38
72	ethanol + methylcyclohexane		8	16.19 kPa	33.69	0.1548	27.39
73	heptane + octane		14	0.02 kPa	0.4	0.0281	0.01
74	1-hexene + 2-butanol		12	0.31 kPa	31	0.1193	11.93
75	hexane + 2-butanol	333.15 K	11	0.33 kPa	32.59	0.1285	12.85
76	methanol + ethyl acetate		15	14.26 kPa	17.31	0.1107	32.09
77	methanol + water	338.15 K	10	47.36 kPa	95.3	0.1581	32.31
78	carbon tetrachloride + 2,2,4—trimethylpentane		6	0.02 kPa	0.82	0.0183	0.01
79	carbon tetrachloride + toluene		16	0.02 kPa	1.07	0.0044	0
80	vinyl acetate + acetic acid	343.15 K	10	2.44 kPa	3.94	0.0307	5.65
81	methyl formate + benzene		12	0.02 kPa	1.61	0.005	0
82	benzene + heptane	353.15 K	13	0.03 kPa	2.6	0.0141	0.01
83	carbon tetrachloride + bromobenzene		21	0.00 kPa	0.23	0.0018	0
84	dimethyl disulfide + toluene	368.15 K	12	11.49 kPa	17.38	0.008	3.15
85	diethyl disulfide + 2,2,4 -trimethylpentane		8	19.98 kPa	31.95	0.0436	17.36
86	pyridine + tetrachloroethylene	373.15 K	19	0.04 kPa	2.62	0.1094	0.04
87	toluene + 1-pentanol	383.15 K	23	0.23 kPa	23.08	0.12	12.45

Note: '-' means that the vapor-liquid phase balance of this system cannot be predicted by the SRK-UNICAC model.

References

1. Chai, M.; Yang, M.; Qi, R.; Chen, Z.; Li, J. Vapor-liquid equilibrium (VLE) prediction for dimethyl ether (DME) and water system in DME injection process with peng-robinson equation of state and composition dependent binary interaction coefficient. *J. Pet. Sci. Eng.* **2022**, *211*, 110172. [CrossRef]
2. Huron, M.J.; Vidal, J. New mixing rules in simple equations of state for representing vapour-liquid equilibria of strongly non-ideal mixtures. *Fluid Phase Equilib.* **1979**, *3*, 255–271. [CrossRef]
3. Wong, D.S.H.; Sandler, S.I. A theoretically correct mixing rule for cubic equations of state. *AIChE J.* **1992**, *38*, 671–680. [CrossRef]
4. Feroiu, V.; Geană, D. Prediction of vapor-liquid equilibria at high pressures using activity coefficients at infinite dilution. *Fluid Phase Equilib.* **1996**, *120*, 1–10. [CrossRef]
5. Iwai, Y. A new activity coefficient model: Simultaneous correlation of liquid-liquid equilibria for ternary systems and vapor-liquid equilibria for constitutive binary systems. *Fluid Phase Equilib.* **2018**, *465*, 24–33. [CrossRef]
6. Iwai, Y.; Seki, R.; Tanaka, Y. Correlation of phase equilibria by new activity coefficient model. *Fluid Phase Equilib.* **2019**, *488*, 62–71. [CrossRef]
7. Yang, Z.L.; Yu, H.Y.; Chen, Z.W. A compositional model for CO_2 flooding including CO_2 equilibria between water and oil using the peng-robinson equation of state with the wong-sandler mixing rule. *Pet. Sci.* **2019**, *16*, 874–889. [CrossRef]
8. Lermite, C.; Vidal, J. High pressure polar compounds phase equilibria calculation: Mixing rules and excess properties. *Fluid Phase Equilib.* **1988**, *42*, 1–19. [CrossRef]
9. Haghtalab, A.; Espanani, R. A new model and extension of wong-sandler mixing rule for prediction of (vapour+ liquid) equilibrium of polymer solutions using EoS/G^E. *J. Chem. Thermodyn.* **2004**, *36*, 901–910. [CrossRef]
10. Michelsen, M.L. A method for incorporating excess Gibbs energy models in equations of state. *Fluid Phase Equilib.* **1990**, *60*, 47–58. [CrossRef]
11. Michelsen, M.L. A modified huron-vidal mixing rule for cubic equations of state. *Fluid Phase Equilib.* **1990**, *60*, 213–219. [CrossRef]
12. Holderbaum, T.; Gmehling, J. PSRK: A group contribution equation of state based on UNIFAC. *Fluid Phase Equilib.* **1991**, *70*, 251–265. [CrossRef]
13. Boukouvalas, C.; Spiliotis, N.; Coutsikos, P. Prediction of vapor-liquid equilibrium with the LCVM model: A linear combination of the vidal and michelsen mixing rules coupled with the original UNIFAC. *Fluid Phase Equilib.* **1994**, *92*, 75–106. [CrossRef]
14. Liu, H.; Li, X.; Wang, Y.; Sun, X.; Zhao, W.; Xia, L.; Xiang, S. Elements and chemical bonds contribution estimation of activity coefficients in nonideal liquid mixtures. *Processes* **2022**, *10*, 2141. [CrossRef]
15. Hou, J.G.; Yang, J.L.; Wang, H.Q. Topology of two-dimensional C60 domains. *Nature* **2001**, *409*, 304–305. [CrossRef]
16. Oteyza, D.; Gorman, P.; Chen, Y.C. Direct imaging of covalent bond structure in single-molecule chemical reactions. *Science* **2013**, *340*, 1434–1437. [CrossRef]
17. Wu, Z.; Shi, L.; Sun, R. A temperature-independent prediction model predicts the vapor-liquid equilibrium of CO_2-based binary mixtures. *Int. J. Refrig.* **2022**, *140*, 125–138. [CrossRef]
18. Xia, L.; Ling, J.Y.; Xu, Z. Application of sequential quadratic programming based on active set method in cleaner production. *Clean Technol. Environ. Policy* **2022**, *24*, 413–422. [CrossRef]
19. Horstmann, S.; Jabłoniec, A.; Krafczyk, J.; Fischer, K.; Gmehling, J. PSRK group contribution equation of state: Comprehensive revision and extension IV, including critical constants and function parameters for 1000 components. *Fluid Phase Equilib.* **2005**, *227*, 157–164. [CrossRef]
20. Li, J.; Xia, L.; Xiang, S.G. A new method based on elements and chemical bonds for organic compounds critical properties estimation. *Fluid Phase Equilib.* **2016**, *417*, 1–6. [CrossRef]
21. Gmehling, J.; Onken, U.; Arlt, W. *Vapor-Liquid Equilibrium Data Collection 34 Parts Dechema Chemistry Data Series*; Starting: Frankfurt, Germany, 1977; Volume I.
22. Erlin, S.; Petri, U.K.; Kari, I.K. Phase equilibria for systems containing dimethyl disulfide and diethyl disulfide with hydrocarbons at 368.15 K. *Fluid Phase Equilib.* **2010**, *293*, 175–181. [CrossRef]
23. Miyamoto, S.; Nakamura, S.; Iwai, Y. Measurement of isothermal vapor—Liquid equilibria for binary and ternary systems containing monocarboxylic acid. *J. Chem. Eng. Data* **2001**, *46*, 1225–1230. [CrossRef]
24. Díez, E.; Rodríguez, A.; Gómez, J.M. Distillation assisted heat pump in a trichlorosilane purification process. *Chem. Eng. Process.* **2013**, *69*, 70–76. [CrossRef]
25. Resa, J.M.; González, C.; Salomé, O.D.L. Density, refractive index, and speed of sound at 298.15 K, and vapor-liquid equilibria at 101.3 kPa for binary mixtures of methanol + ethyl butyrate and vinyl acetate + ethyl butyrate. *J. Chem. Eng. Data* **2002**, *47*, 1123–1127. [CrossRef]
26. Trandaflr, R.; Llvlu, S. Isobaric vapor-liquid equilibria for the binary systems CH_3SiHCl_2 with $(CH_3)_3SiCl$, $(CH_3)_2SiCl_2$, CH_3SiCl_3, or $SiCl_4$. *J. Chem. Eng. Data* **1992**, *37*, 143–145. [CrossRef]
27. Yang, B.L.; Wang, H.J. Vapor-liquid equilibrium for mixtures of water, alcohols, and ethers. *J. Chem. Eng. Data* **2002**, *47*, 1324–1329. [CrossRef]
28. Masashi, T.; Ryo, K.; Hideo, N. Henry's law constant measurements of CCl_2F_2, $CHClF_2$, CH_2F_2, C_2ClF, C_2HF, CH_2FCF_3, and CH_3CHF_2 in methanol, ethanol, and 2-propanol. *J. Chem. Eng. Data* **2001**, *46*, 746–749. [CrossRef]
29. Jakob, A.; Grensemann, H.; Lohmann, J.; Gmehling, J. Further development of modified UNIFAC (Dortmund): Revision and extension 5. *Ind. Eng. Chem. Res.* **2006**, *45*, 7924–7933. [CrossRef]

30. Larsen, B.L.; Rasmussen, P.; Fredenslund, A. A modified UNIFAC group-contribution model for prediction of phase equilibria and heats of mixing. *Ind. Eng. Chem. Res.* **1987**, *26*, 2274–2286. [CrossRef]
31. Wittig, R.; Lohmann, J.; Gmehling, J. Vaporliquid equilibria by UNIFAC group contribution. 6. revision and extension. *Ind. Eng. Chem. Res.* **2003**, *42*, 183–188. [CrossRef]
32. Tochigi, K.; Gmehling, J. Determination of ASOG parameters-extension and revision. *J. Chem. Eng.* **2011**, *44*, 304–306. [CrossRef]